Process Safety and Environmental Protection 168 (2022) 434–442

Contents lists available at ScienceDirect

Process Safety and Environmental Protection

journal homepage: www.journals.elsevier.com/process-safety-and-environmental-protection

LED visible light assisted photochemical oxidation of HCHs in aqueous phases polluted with DNAPL

Leandro O. Conte [a,b], Salvador Cotillas [a], Andrés Sánchez-Yepes [a], David Lorenzo [a], Aurora Santos [a,*]

[a] Department of Chemical Engineering and Materials, Faculty of Chemical Sciences, Complutense University of Madrid, Avenida Complutense s/n, 28040 Madrid, Spain
[b] Instituto de Desarrollo Tecnológico para la Industria Química (INTEC), Consejo Nacional de Investigaciones Científicas y Técnicas (CONICET) and Universidad Nacional del Litoral (UNL), Ruta Nacional N 168, 3000 Santa Fe, Argentina

ARTICLE INFO

Keywords:
DNAPL
Lindane
Persulfate
Ferrioxalate
LED Vis-Light

ABSTRACT

This work focuses on removing hexachlorocyclohexanes (HCHs) found in groundwater polluted with dense non-aqueous phase liquids (DNAPLs) by photo-oxidation with hydrogen peroxide or persulfate using LED visible light and ferrioxalate as the catalyst. Single oxidation tests were also performed to evaluate the contribution of LED-vis light on HCHs removal. Results show that it is possible to attain the degradation of HCHs up to 85% in 420 min with persulfate, whereas percentages lower than 40% are obtained when using hydrogen peroxide. Using both oxidants in the presence of ferrioxalate and LED visible light promotes the generation of hydroxyl and sulfate radicals under circumneutral pH values, which are the main responsible species for HCHs removal. Specifically, an oxidant conversion higher than 50% was achieved during the photochemical treatment with both oxidants, whereas conversions below 20% were obtained in the absence of LED visible light irradiation. On the other hand, DNAPL produced as liquid residuum of lindane production contains other chlorinated organic compounds (COCs), which are susceptible to being oxidized by hydroxyl and sulfate radicals, generating competitive oxidation reactions. The final conversion of chlorbenzenes reaches values close to 100% and HCHs are only effectively removed when persulfate is used as the oxidant. This better performance indicates that the photo-oxidation of DNAPL polluted groundwater with LED-vis light should be carried out with persulfate to ensure the removal of more dangerous COCs. This confirms the excellent ability of sulfate radicals for C-Cl bond breakdown.

1. Introduction

The occurrence of chlorinated organic compounds (COCs) from dense non-aqueous phase liquids (DNAPLs) in groundwater is a significant concern for the scientific community due to the hazards associated to this type of compounds (Campanale et al., 2021; Jiao et al., 2009). DNAPLs come from accidental spills, leakages or uncontrolled discharges in different industrial activities (Birak and Miller, 2009; Güler, 2019; Wang et al., 2014). In particular, groundwater contaminated by chlorinated compounds in two industrial landfills (Bailin and Sardas) in Sabiñanigo (Spain) is considered here. High amounts of DNAPLs from lindane (γ-hexachlorocyclohexane, γ-HCH) production were dumped in unlined landfills for several decades in the twentieth century (Fernández et al., 2013; Santos et al., 2018). This DNAPL contains 28 different COCs, including different isomers of hexachlorocyclohexane (HCH). These compounds are solubilized in groundwater (Lorenzo et al., 2020). For this reason, it is necessary to develop clean and efficient technologies that remove COCs from water bodies.

In this context, Advanced Oxidation Processes (AOPs) can be considered a suitable alternative for removing COCs from groundwater. Fenton oxidation is a well-known AOP that promotes the generation of hydroxyl radicals by activating hydrogen peroxide with ferrous iron (Eq. 1).

$$H_2O_2 + Fe^{2+} \rightarrow \cdot OH + OH^- + Fe^{3+} \quad (1)$$

The iron catalyst can be regenerated during the Fenton process by the reaction between ferric iron and hydrogen peroxide (Eqs. 2–3). However, the kinetic constant of reaction in Eq. (1) is significantly higher than that for Eq. (2) (Malato et al., 2009).

* Corresponding author.
E-mail address: aursan@ucm.es (A. Santos).

https://doi.org/10.1016/j.psep.2022.10.015
Received 29 July 2022; Received in revised form 7 October 2022; Accepted 7 October 2022
Available online 12 October 2022

$$Fe^{3+} + H_2O_2 \rightarrow H^+ + Fe(HO_2)^{2+} \quad (2)$$

$$Fe(HO_2)^{2+} \rightarrow Fe^{2+} + HO_2 \quad (3)$$

The efficiency of Fenton oxidation can be improved by coupling UV light (photo-Fenton) because the irradiation of UVA light ($315 < \lambda < 400$) over an iron complex ($Fe(OH)^{2+}$) previously formed during the process (Eq. 4) promotes an increase in the production of hydroxyl radicals and accelerate the recovery of Fe^{2+} from Fe^{3+} (Ebrahiem et al., 2017).

$$[Fe(OH)^{2+}] + h\nu \rightarrow Fe^{2+} + \cdot OH \quad (4)$$

Recent works reported in the literature have informed that the ability of hydroxyl radicals to remove aliphatic compounds can be limited (Mena et al., 2018; Varanasi et al., 2018). For this reason, other radicals have been studied to remove organic pollutants that ensure the elimination of both aromatics and aliphatics. Specifically, the sulfate radical has been proven efficient for completely removing organic pollutants and their mineralization (Giannakis et al., 2021; Lian et al., 2017). This radical can be obtained from persulfate activation by transition metal ions (Wang and Wang, 2018). The use of ferrous iron in the presence of persulfate promotes the rapid production of sulfate radicals ($k_{22\,°C} = 20\ M^{-1}\ s^{-1}$) (Eq. 5) and the subsequent oxidation of organic pollutants (Anipsitakis and Dionysiou, 2004; Wacławek et al., 2017).

$$S_2O_8^{2-} + Fe^{2+} \rightarrow SO_4^{\cdot-} + SO_4^{2-} + Fe^{3+} \quad (5)$$

Regeneration of Fe^{2+} from Fe^{3+} cannot be achieved by the reaction between persulfate and Fe^{3+}. To overcome this limitation, persulfate photo-assisted processes have been recently proposed to maintain the radical production by recovering ferrous iron (Eq. 4) (Graça et al., 2017; Rao et al., 2021).

The light source is a critical input for developing high-efficient and low-cost photo-assisted technologies. The use of wavelengths around 254 nm (UVC) significantly improves the degradation rate of pollutants during photo-assisted processes because it promotes not only the photoactivation of iron (Eq. 4) but also the dissociation of hydrogen peroxide and persulfate (Eqs. 6–7), increasing the production of hydroxyl and sulfate radicals, respectively (Díaz-Angulo et al., 2021; Rao et al., 2021).

$$H_2O_2 + h\nu \rightarrow 2\ OH \quad (6)$$

$$S_2O_8^{2-} + h\nu \rightarrow 2\ SO_4^{\cdot-} \quad (7)$$

However, the energy costs of this artificial light are very high. For this reason, lower wavelengths have been tested to obtain artificial lights close to visible solar radiation during photo-assisted technologies (Babuponnusami and Muthukumar, 2014). LED lights have been employed to remove organic pollutants due to reduce heat dissipation (Carra et al., 2015).

Furthermore, using iron salts with both oxidants (H_2O_2 or $S_2O_8^{2-}$), the pH of the media should be maintained at values around 3 to ensure the total dissolution of iron (Díez et al., 2018; Rodriguez et al., 2014). Nonetheless, several authors have proposed using citrate- or oxalate-based iron complexes to develop homogeneous photo-assisted processes under pH values close to the neutrality (Graça et al., 2017; Nogueira et al., 2017; Santos-Juanes et al., 2017).

With this background, this work aims to evaluate the removal of HCHs from DNAPL saturated groundwater extracted from subsoil for the first-time using persulfate and ferrioxalate photo-assisted by LED-vis light (470 nm) as an on-site technology. Likewise, hydrogen peroxide as an oxidant is also studied, and the efficiencies of both processes are compared in the presence or absence of light irradiation. To the author's knowledge, the use of LED-vis lights emitting at wavelengths within the visible solar light zone for the degradation of HCHs in homogeneous systems using an oxalate-based iron complex has not yet been reported. This could decrease the energy requirements of the photo-assisted processes since visible light represents almost 50% of solar light (Lorenzo et al., 2021). In addition, this is a topic of great interest because of the hazardousness of these pollutants.

2. Material and methods

2.1. Chemicals

DNAPL samples were obtained from the Sabiñánigo landfills and were kindly provided by the company EMGRISA and the Government of Aragon (Spain). Hydrogen peroxide (35 wt%) and sodium persulfate (98%) were used as oxidants (Sigma Aldrich, Spain). Potassium oxalate monohydrate (99.5%) and iron (III) sulfate hydrate (97%) were employed for the formulation of the ferrioxalate complex (Sigma Aldrich, Spain). N-hexane used for the extraction of COCs was provided by Scharlau, Spain. Tetrachloroethane and butyl cyclohexane (Sigma Aldrich, Spain) were used as standard internal compounds to quantify COCs in the ECD and FID detectors, respectively. The determination of hydrogen peroxide and persulfate required titanium oxysulfate and sodium thiosulfate, respectively. Sodium carbonate, sodium bicarbonate, sulphuric acid, oxalic acid, and acetone were used to measure chlorides. 1,10-phenanthroline and sodium acetate used to determine iron and sodium hydroxide employed for pH adjustment were purchased by Sigma Aldrich (Spain). All the stock solutions were prepared with high-purity water from a Millipore Direct-Q system (resistivity>18 MΩ cm at 25 ºC).

2.2. Experimental procedure

All the experiments were conducted in an isothermal double-walled cylindrical batch reactor ($V_T = 0.10$ L) equipped with a magnetic stirring system (IKA C-MG HS 7, Staufen, Germany). The temperature was kept constant at 25 ºC using a thermostatic bath. Polluted water saturated in DNAPL was illuminated with a collimated LED of Migthtex (high-power LCS-0470–50–11, Lasing, Spain) located at the top of the reactor (emission peak at 470 nm). The collimator light sources produce an optical power output of up to 4.17 W, and the power could be adjusted manually using a Migthtex LED controller. The light LED source emits over the reactor window with an irradiated area of 11 cm^2. More details of the reaction device have been described elsewhere, but during the removal of 1,2,4-trichlorobenzene by heterogeneous catalytic wet peroxide oxidation (Lorenzo et al., 2021).

Synthetic groundwater saturated with DNAPL was prepared by dissolving 1 g of DNAPL in a ferrioxalate solution without headspace to avoid the possible evaporation of COCs. The ferrioxalate solution (oxalate/iron molar ratio of 10:1) was prepared according to the methodology described by Murov et al. (1993). The resulting solution (ferrioxalate + DNAPL) was agitated for 24 h and kept at room temperature (23 °C ± 2 °C). It was experimentally confirmed that equilibrium between the organic and aqueous phase was obtained at times lower than 24 h with a stable concentration of COCs in the aqueous phase at 24 h. DNAPL saturated groundwater containing the ferrioxalate complex was added to the reactor, followed by the pH adjustment to 6.5 using a concentrated NaOH solution. The first sample was taken after adding the oxidant, and the lamp shutter was removed to start the experiment. The oxidant dose was twice the stoichiometric dose to ensure enough concentration in the effluent to remove the total organic matter. The chemical composition of the simulated DNAPL polluted groundwater was reported elsewhere (Santos et al., 2018). Samples were collected from the reactor and immediately extracted with n-hexane (0.3 mL n-hexane + 1.2 mL sample) to stop the reaction and measure the concentration of COCs.

2.3. Analyses

The COCs concentrations were quantified by gas chromatography (Agilent, USA) equipped with a Flame Ionisation Detector (FID) and an Electron Capture Detector (ECD). Compounds have been previously identified by GC/MSD (Santos et al., 2018). The aqueous phase (1.2 mL) was extracted with n-hexane (0.3 mL), and the mixture of both phases was shaken, followed by settlement, allowing the organic phase separation by decantation. An HP-5MS column ((5%-phenyl)--methylpolysiloxane, 30 m × 0.25 mm ID x 0.25 μm) was used as a stationary phase, and a constant flow rate of 1.7 mL min^{-1} He was used as a mobile phase. The oven worked under a predetermined temperature gradient, starting at 80 °C and increasing the temperature at a rate of 18 °C min^{-1} up to 180 °C, then keeping it constant for 15 min. Butyl cyclohexane and tetrachloroethane were added to the samples as internal standards (ISTDs) for FID and ECD analyses, respectively, to reduce experimental errors in COCs quantification (Santos et al., 2018). The persulfate concentration was determined by a colorimetric method with sodium bicarbonate and potassium iodide, using a BOECO S-20 UV–VIS spectrophotometer at 352 nm (Liang et al., 2008). 50 μL sample were added to 10 mL of a stock solution containing 5 g/L $NaHCO_3$ and 100 g/L KI. The resulting solution was then measured spectrophotometrically after 15 min of reaction. Hydrogen peroxide concentration was measured by a standard method using titanium(IV) oxysulfate (Eisenberg, 1943). It consists of adding 0.5 mL sample to 4.5 mL ultrapure water and 0.5 mL of a stock solution of titanium(IV) oxysulfate (2%). The resulting solution was measured by spectrophotometry at 410 nm. Total iron concentration was also determined spectrophotometrically using 1,10-phenanthroline (510 nm) (Conte et al., 2016). Chlorides were measured by an ion chromatograph equipped with a conductivity detector (Metrohm 930 Compact IC Flex). A Metrosep A Supp 5–250/4.0 column (25 cm x 4 mm ID) was used, and the mobile phase was a solution of 3.2 mM Na_2CO_3 + 1 mM $NaHCO_3$ with a flow rate of 0.7 mL min^{-1}. The pH was measured with a Basic 20-CRISON electrode (Barcelona, Spain). The irradiance and radiation flux of the LED lamp were measured using a Flame UV–VIS spectrometer (Ocean Insight, The Netherlands). The conversion of all species involved in the technologies employed was calculated following the Eq. 8, where X_j is the conversion of the species j, C_j is the concentration (mmol/L) of the species j at a given time, and C_{j0} is the initial concentration (mmol/L) of the species j.

$$Xj = 1\text{-}\ (C_j/C_{j0}) \quad (8)$$

3. Results and discussion

The composition of COCs in saturated water with DNAPL is shown in Table 1. This composition is similar to that found in the groundwater of several wells of the Sardas and Bailin Landfills (Santos et al., 2018).

Twenty different COCs were identified in the effluent, being the concentration of chlorobenzene and HCHs higher than the values obtained for other COCs. According to this initial composition, the theoretical concentration of hydrogen peroxide and persulfate required to attain the complete mineralization of all COCs is 7.5 mM, respectively. The oxidant stoichiometric ratio employed for the development of photo-assisted technologies was 1:1. Fig. 1 shows the conversion of HCHs in polluted water with the reaction time during the chemical oxidation and photo-oxidation of synthetic groundwater saturated with DNAPL using hydrogen peroxide and persulfate.

The catalyst employed during all processes was a ferrioxalate complex with an oxalate/iron molar ratio of 10:1 to avoid the precipitation of iron species and keep them in solution. Under these conditions, the dominant ferrioxalate complex is $Fe^{III}(C_2O_4)_3^{3-}$ (96.25%) (Visual MINTEQ version 3.0, USEPA). This organic complex has higher molar radiation absorption coefficients in the UV-Vis region than the aqueous iron complexes (Conte et al., 2014). Furthermore, it allows the use of iron concentrations below the discharge limit established by, among others, the Spanish legislation (0.18 mM) (del Estado, 2018), avoiding its subsequent removal.

No conversion of HCHs was observed during the oxidation with hydrogen peroxide and ferrioxalate in the absence of light irradiation (Fig. 1a). This behaviour can be due to the lower production of free hydroxyl radicals in the effluent since the reaction between hydrogen peroxide, and ferrioxalate is very slow (Eq. 9) (Conte et al., 2019). On the other hand, using persulfate and ferrioxalate leads to final conversions of HCHs of about 60% (Fig. 1b) in the absence of light. This reveals the critical role of the nature of the oxidant on the removal efficiency of HCHs. The production of sulfate radicals seems to occur also under dark conditions and, hence, the subsequent degradation of HCHs (Eq. 10).

$$H_2O_2 + Fe^{III}(C_2O_4)_3^{3-} \rightarrow Fe^{II}(C_2O_4) + 2\ C_2O_4^{2-} + \cdot OH + OH^- \quad (9)$$

$$S_2O_8 + Fe^{III}(C_2O_4)_3^{3-} \rightarrow Fe^{II}(C_2O_4) + 2\ C_2O_4^{2-} + SO_4^{\cdot -} + SO_4^{2-} \quad (10)$$

The irradiation of LED-vis light to the reactor significantly enhances

Table 1
COCs contained in DNAPL polluted groundwater.

Name	Formula	Molecular weight (g mol^{-1})	Concentration (mg L^{-1})	Concentration (mmol L^{-1})
Chlorobenzene (CB)	C_6H_5Cl	112.56	28.27 ± 4.03	0.25 ± 0.04
1,3-dichlorobenzene (1,3-DCB)	$C_6H_4Cl_2$	147.01	0.26 ± 0.06	0.002 ± 0.0004
1,4-dichlorobenzene (1,4-DCB)			2.79 ± 0.11	0.02 ± 0.0007
1,2-dichlorobenzene (1,2-DCB)			2.03 ± 0.06	0.01 ± 0.0004
1,3,5-trichlorobenzene (1,3,5-TCB)	$C_6H_3Cl_3$	181.45	0.02 ± 0.01	0.0001 ± 0.00006
1,2,4-trichlorobenzene (1,2,4-TCB)			7.97 ± 5.51	0.04 ± 0.03
1,2,3-trichlorobenzene (1,2,3-TCB)			0.19 ± 0.01	0.001 ± 0.00006
(1,2,3,4 + 1,2,4,5)-tetrachlorobenzene (1,2,3,4 + 1,2,4,5-TetraCB)	$C_6H_2Cl_4$	215.89	0.24 ± 0.03	0.001 ± 0.0001
1,2,3,5-tetrachlorobenzene (1,2,3,5- TetraCB)			0.35 ± 0.08	0.002 ± 0.0004
γ-pentachlorocyclohexene (γ-PCX)	$C_6H_5Cl_5$	254.25	2.24 ± 0.49	0.009 ± 0.002
δ- pentachlorocyclohexene (δ-PCX)			3.22 ± 0.37	0.013 ± 0.001
θ- pentachlorocyclohexene (θ-PCX)			0.58 ± 0.01	0.002 ± 0.00004
β- pentachlorocyclohexene (β-PCX)			0.62 ± 0.11	0.002 ± 0.0004
η- pentachlorocyclohexene (η-PCX)			3.13 ± 0.96	0.012 ± 0.004
α-hexachlorocyclohexane (α-HCH)	$C_6H_6Cl_6$	290.83	1.70 ± 0.26	0.006 ± 0.0009
γ-hexachlorocyclohexane (γ-HCH)			8.35 ± 1.56	0.029 ± 0.005
δ-hexachlorocyclohexane (δ-HCH)			15.24 ± 3.40	0.05 ± 0.01
ε-hexachlorocyclohexane (ε-HCH)			1.12 ± 0.23	0.004 ± 0.0008
Heptachlorocyclohexane-1 (HeptaCH-1)	$C_6H_5Cl_7$	325.28	0.73 ± 0.30	0.002 ± 0.0009
Heptachlorocyclohexane-2 (HeptaCH-2)			0.25 ± 0.23	0.0008 ± 0.0007
∑COCs			79.33 ± 17.82	0.4559 ± 0.0979

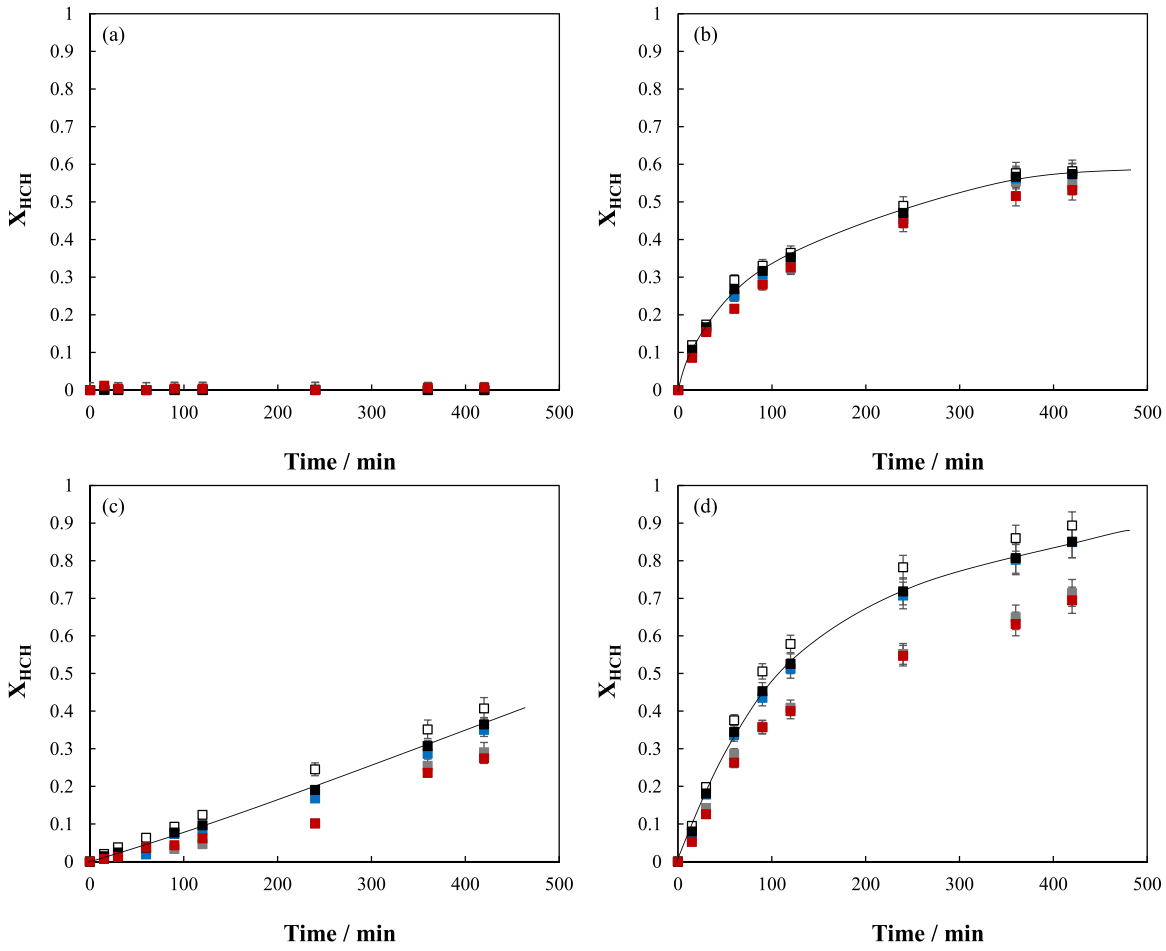

Fig. 1. Conversion of HCHs as function of the operation time during the photo-oxidation of groundwater saturated with DNAPL. (a) H_2O_2/Fe; (b) $Na_2S_2O_8$/Fe; (c) H_2O_2/Fe/LED; (d) $Na_2S_2O_8$/Fe/LED; (□) α-HCH; (□) γ-HCH; (■) δ-HCH; (■) ε-HCH; (■) Total HCHs; $[Fe]_0$: 0.13 mM; $[H_2O_2]_0$: 7.5 mM; $[Na_2S_2O_8]_0$: 7.5 mM; I_{LED}: 0.18 W cm^{-2}; T: 25 ºC; pH_0: 6.5.

the removal of HCHs with both oxidants. However, the conversion of the total HCHs is about 40% when hydrogen peroxide is used as an oxidant (Fig. 1c), whereas it increases above 80% with persulfate (Fig. 1d) within 420 min of reaction. These results again highlight the importance of the type of oxidant in removing HCHs. Using persulfate and ferrioxalate without LED-vis light (Fig. 1b) attains higher conversions than the photo-Fenton process (Fig. 1c). Specifically, δ- and γ-HCH achieved the highest conversion values, followed by α- and ε-HCH. This is an expected behaviour considering the previous results reported in the literature during the removal of these organochlorinated compounds by advanced oxidation processes where the oxidants attack the pollutants, reaching different degradation efficiencies depending on the position of the chlorine atoms (Dominguez et al., 2021).

The removal of HCHs occurs by the action of free radicals generated from activating the oxidants. The irradiation with LED Vis-Light during Fenton oxidation (photo-Fenton) leads to the generation of higher amounts of hydroxyl radicals through the photo-activation of an iron complex previously formed (Eq. 4), increasing the removal rate of organics (Babuponnusami and Muthukumar, 2014). Likewise, persulfate can be easily decomposed into sulfate radicals by reacting with iron (Eq. 6) (Rodriguez et al., 2017). These radicals present a high oxidation potential close to hydroxyl radicals (2.6 vs. 2.8 V), favouring the depletion of organic pollutants in water (Ioannidi et al., 2022; Milh et al., 2021; Xiao et al., 2020). The occurrence of both radicals by the activation of the parent oxidants with iron has been reported in the literature by using scavenger species such as benzoquinone, tert-butyl alcohol or isopropanol (Khajone et al., 2019; Khajone and Bhagat, 2020; Kordestani et al., 2019).

The differences observed in conversion profiles with both oxidants are directly related to the different mechanisms of hydroxyl and sulfate radicals to attack these pollutants (Khan et al., 2021). The first ones promote addition reactions and hydrogen abstraction, whereas sulfate radicals favour the electron transfer reaction (Wacławek et al., 2019). Hence, hydroxyl radicals attack the C-H bond, and sulfate radicals break the C-Cl bond. The energy of the C-H bond is higher than that of the C-Cl bond (97 vs 79 KJ mol^{-1}), and the selectivity of sulfate radical is higher than hydroxyl radical (Khan et al., 2017). This results in a more favoured attack of sulfate radicals on HCHs.

Hydrogen peroxide and persulfate concentrations were monitored during the oxidation and photo-oxidation of synthetic groundwater saturated with DNAPL. The conversion of both oxidants with the operation time is plotted in Fig. 2. Free hydroxyl and sulfate radicals generation can be correlated with the oxidant conversion.

As expected, a very low conversion of hydrogen peroxide was observed during the process in the absence of light since the conversion of HCHs was negligible (Fig. 1a). However, the conversion of persulfate reached a final value of 0.18 in the oxidation tests without light irradiation. This confirms the production of free sulfate radicals during the reaction between persulfate and ferrioxalate (Eq. 10). During photo-oxidation tests, the final conversions of hydrogen peroxide and persulfate were 0.55 and 0.58, respectively.

These results show that persulfate activation is higher than hydrogen peroxide activation in the absence of light. In the presence of light, PS and H_2O_2 conversions are closer, but PS conversion is slightly higher;

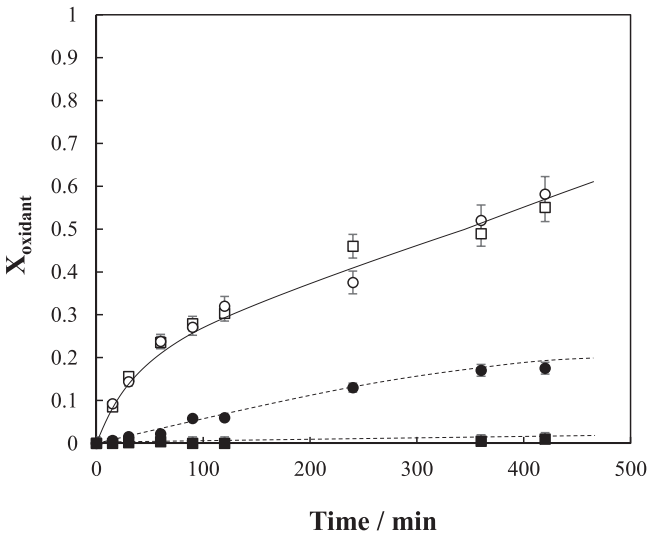

Fig. 2. Conversion of oxidants with reaction time during the oxidation and photo-oxidation of groundwater saturated with DNAPL. (■) H_2O_2/Fe; (●) $Na_2S_2O_8$/Fe; (□) H_2O_2/Fe/LED; (○) $Na_2S_2O_8$/Fe/LED; $[Fe]_0$: 0.13 mM; $[H_2O_2]_0$: 7.5 mM; $[Na_2S_2O_8]_0$: 7.5 mM; I_{LED}: 0.18 W cm^{-2}; T: 25 ºC.

therefore, the concentration of sulfate radicals is expected to be higher than the amount of hydroxyl radicals. The values of the kinetic constants reported in the literature for the activation of hydrogen peroxide and persulfate by ferrous iron are 70 and 20 $M^{-1}s^{-1}$, respectively (Matzek and Carter, 2016; Neyens and Baeyens, 2003). The production rate of hydroxyl radicals is expected to be 3.5 times higher than the generation of sulfate radicals under dark conditions. Hence, the low conversion of hydrogen peroxide could be related to the possible recombination of hydroxyl radicals in the effluent, promoting the generation of hydrogen peroxide and the subsequent decrease in HCHs removal efficiency (Eq. 11).

$$OH + \cdot OH \rightarrow H_2O_2 \quad (11)$$

At this point, it is essential to note that the iron employed as a catalyst in this work is in ferrioxalate form, and it is expected that the kinetic constants of radical generation reactions in the presence of LED-vis light may be different from the values reported in the literature with ferrous iron under dark conditions.

The similar conversion of both oxidants in the presence of light does not result in similar HCHs conversion, as shown in Fig. 1, where the conversion of HCHs is higher when using persulfate, confirming the better efficiency of sulfate radicals on HCHs degradation. This can also be confirmed by comparing the HCHs conversion obtained with persulfate in the absence of light with the conversion achieved with hydrogen peroxide in the photo-Fenton process. Higher conversions of HCHs (Fig. 1b) are obtained with PS and the absence of light than with hydrogen peroxide in the light presence (Fig. 1b), despite higher oxidant conversions being obtained in the first case (Fig. 2). The different behaviour observed in both oxidants against HCHs could be related to the different mechanisms of attack on HCHs.

On the other hand, oxidation reactions take place at pH values around 6. Under these conditions, iron salts may precipitate in the aqueous media; however, no precipitates were observed during the oxidation and photo-oxidation treatments, regardless of the oxidant used. This reveals that the iron-based complex (ferrioxalate) employed to remove HCHs from synthetic groundwater saturated with DNAPL is suitable for keeping iron in solution at circumneutral pH.

As shown in Table 1, DNAPL contains not only HCHs but also other chlorinated organic compounds (COCs), such as chlorobenzene (CB), dichlorobenzene (DCBs), trichlorobenzenes (TCBs), tetrachlorobenzenes (TetraCBs), pentachlorocyclohexenes (PentaCXs) and heptachlorocyclohexanes (HeptaCHs), which are also solubilized in the aqueous phase and can consume radicals during the process. The concentration of COCs was analysed, and their conversion is shown in Fig. 3 with the operation time during the oxidation and photo-oxidation of synthetic groundwater saturated with DNAPL.

As can be observed, COC conversion increases with time during oxidation and photo-oxidation tests carried out, regardless of the oxidant used. This confirms that hydroxyl and sulfate radicals effectively remove other chlorinated organics but HCHs; hence, competitive oxidative reactions exist between HCHs and other COCs contained in DNAPL during the process. Nonetheless, the efficiencies obtained with each oxidant are different. In the case of hydrogen peroxide (Fig. 3a), the conversion of CB and DCBs is between 80% and 90%, whereas the values obtained for TCBs, TetraCBs and PCXs were 40%, 15% and 18%, respectively. The irradiation of LED-vis light improves COCs conversion (Fig. 3c). Specifically, the conversion of CB and DCBs was higher than 90%, and TCBs, TetraCBs and PCXs achieved final conversions of 62%, 52% and 55%, respectively. HeptaCHs seem to be not affected by the presence of hydroxyl radicals in the aqueous media (null conversion), regardless of the technology employed. The lower the number of chlorines in the molecule, the higher the conversion. This again indicates that the C-Cl bond is difficult to break by hydroxyl radicals since the degradation efficiency decreases when the number of chlorine atoms increases, i.e., the number of C-Cl bonds (Khan et al., 2017, 2021). The results obtained during the oxidation with hydrogen peroxide and ferrioxalate (Fig. 3a) are unexpected since the conversion of the oxidant was low (Fig. 2). This suggests that the COCs with a low molecular weight than HCHs could be removed not only by oxidation but also by evaporation.

Similar behaviour can be seen regarding the evolution of COCs with persulfate. The final conversion of CB, DCBs, TCBs, TetraCBs, PCXs and HeptaCHs during the oxidation tests in the light absence were 0.92, 0.81, 0.79, 0.60, 0.59 and 0.1, respectively (Fig. 3b). The light enhances these values, achieving complete removal of CB, DCBs, TCBs, TetraCBs and PCXs in 420 min. The conversion of HeptaCHs reaches around 80% when LED-vis light is irradiated (Fig. 3d). These results reveal the importance of LED-vis light for generating large amounts of free radicals and the subsequent removal of organics. At 60 min, the conversion of COCs in the photo-oxidation with persulfate (Fig. 3d) is close to the values obtained during the process with hydrogen peroxide in 420 min (Fig. 3c). These higher efficiencies reveal that sulfate radicals attack the COCs more rapidly than hydroxyl radicals, including HCHs (Fig. 1).

As commented above, the COCs conversions achieved during the oxidation and photo-oxidation of synthetic groundwater saturated with DNAPL could be related not only to the oxidation or photo-oxidation of the pollutants but also to the evaporation process. For this reason, evaporation tests were performed by monitoring the COCs concentration in synthetic groundwater saturated with DNAPL without oxidant and catalyst under dark conditions but in the same experimental set-up. Results are plotted in Fig. 4.

As shown in Fig. 4, the decrease of COCs in the aqueous phase with less than five chlorine atoms increases over time. Specifically, the final value of CB, DCBs, TCBs and TetraCBs was 0.70, 0.52, 0.45 and 0.31 of their initial values, respectively. PCXs, HCHs and HeptaCHs do not modify their concentrations with time. This confirms that low molecular weight COCs are easily removed by evaporation in the experimental system. Hence, the conversions of these compounds obtained during the oxidation and photo-oxidation processes involve oxidation and evaporation processes. To evaluate the contribution of each process to the COCs removal, it is necessary to know the moles removed by oxidation and evaporation with time. They can be calculated by the Eq. 12, considering a first-order kinetic model

$$-\frac{dN_j}{dt} = \frac{dn_{j\,ox}}{dt} + \frac{dn_{j\,ev}}{dt} = k_{oxj}\cdot C_j\cdot V_L + k_{evj}\cdot C_j\cdot V_L \quad (12)$$

where N_j are the moles of the j compound in the reaction media at a

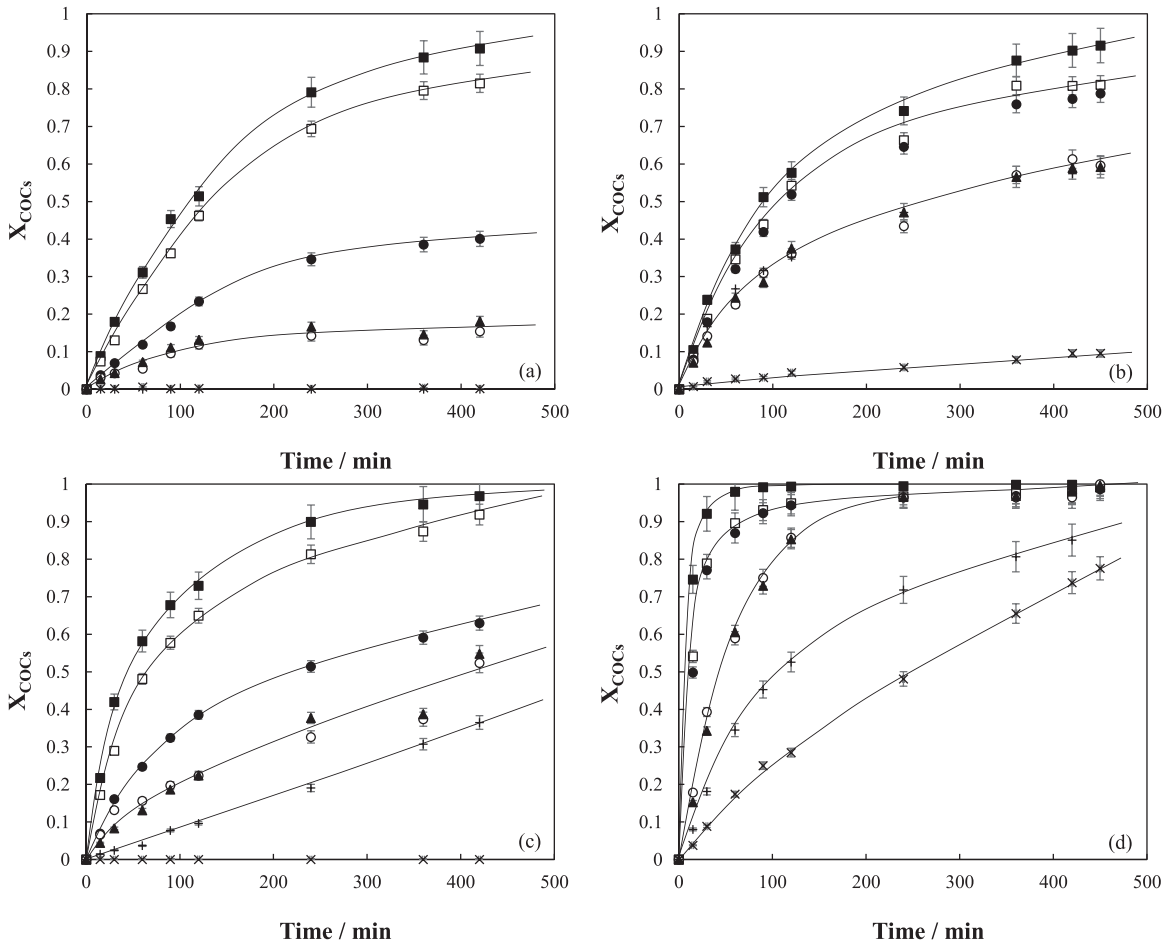

Fig. 3. Conversion of COCs as function of the operation time during the oxidation and photo-oxidation of groundwater saturated with DNAPL. (a) H_2O_2/Fe; (b) $Na_2S_2O_8$/Fe; (c) H_2O_2/Fe/LED; (d) $Na_2S_2O_8$/Fe/LED; (■) CB; (□) DCBs; (●) TCBs; (○) TetraCBs; (▲) PCXs; (+) HCHs; (x) HeptaCHs; $[Fe]_0$: 0.13 mM; $[H_2O_2]_0$: 7.5 mM; $[Na_2S_2O_8]_0$: 7.5 mM; I_{LED}: 0.18 W cm^{-2}; T: 25 ºC.

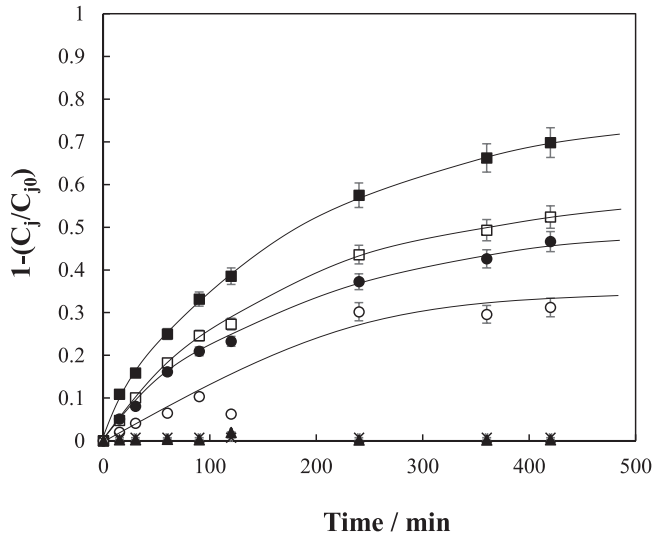

Fig. 4. Conversion of COCs as a function of the operation time during the evaporation of groundwater saturated with DNAPL. (■) CB; (□) DCBs; (●) TCBs; (○) TetraCBs; (▲) PCXs; (+) HCHs; (x) HeptaCHs; T: 25 ºC.

given time (t), $n_{j\ ox}$ the moles of j oxidized from zero to t, and $n_{j\ ev}$ the moles of j evaporated from zero to t, k_{oxj} and k_{evj} the kinetic constant for the oxidation and evaporation of the compound j, respectively. C_j is the concentration of j in the aqueous phase at the time t and V_L is the volume of the aqueous phase. C_j can be expressed as a function of the initial moles of j (N_{jo}) and the disappeared moles by the sum of evaporation and oxidation contributions (Eq. 13).

$$C_j = \frac{N_j}{V_L} = \frac{N_{j0} - n_{j_{ev}} - n_{j_{ox}}}{V_L} \quad (13)$$

Contribution of evaporation and oxidation to the disappearance of the compound j with the time can be calculated by Eqs. 14 and 15, respectively:

$$X_{j_{ox}} = \frac{n_{j\ ox}}{N_{jo}} = \frac{k_{oxj}}{k_{oxj} + k_{evj}}\left(1 - exp\ \left(-k_j \cdot t\right)\right) \quad (14)$$

$$X_{j_{ev}} = \frac{n_{j\ ev}}{N_{jo}} = \frac{k_{evj}}{k_{oxj} + k_{evj}}\left(1 - exp\ \left(-k_j \cdot t\right)\right) \quad (15)$$

Finally, the total disappearance of compound j involves both processes: evaporation and oxidation (Eq. 16).

$$X_j = \frac{N_{jo} - N_j}{N_{jo}} = \frac{k_{oxj}}{k_{oxj} + k_{evj}}\left(1\text{-}exp\ \left(-k_j \cdot t\right)\right) + \frac{k_{evj}}{k_{oxj} + k_{evj}}\left(1\text{-}exp\ \left(-k_j \cdot t\right)\right) \quad (16)$$

The kinetic constant k_{evj} of each j compound has been obtained from Fig. 4 and equation 15 ($k_{oxj} = 0$; $k_{evj} = k_j$). Likewise, the kinetic constant k_{oxj} for each j compound has been obtained from Fig. 3 and equation 16,

with known values of k_{evj}. The correlation coefficients (R^2) of k_j and k_{evj} were higher than 0.98 in all cases analysed. Table 2 shows the oxidation kinetic constants obtained for all COCs, with both oxidants, in the presence and absence of light.

As can be observed, the kinetic constants for CB and DCBs are low and quite similar in the absence of light with both oxidants, revealing that the evaporation process is promoted over oxidation. This is more remarkable in the case of TCBs and TetraCBs with hydrogen peroxide, where a null oxidation kinetic constant was obtained. These results indicate that chlorobenzenes evaporate rapidly. Light irradiation enhances the kinetic constants with both oxidants, although the highest values were obtained during the process with persulfate. Overall, the oxidation kinetic constants decrease when increasing the molecular weight of the COCs. This suggests that the number of C-Cl bonds influences the degradation rate. TetraCBs show a very low value of the oxidation kinetic constant in most of the tests performed, which could be related to the low initial concentration of these compounds in the effluents (Table 1). To evaluate the real contribution of evaporation and oxidation processes on the degradation of COCs, the conversions of both processes were calculated following Eqs. 14 and 15. These values are only given for chlorobenzenes because they are the COCs susceptible to evaporation (Fig. 4). Table 3 shows the total, oxidation and evaporation conversion of each COC during the oxidation and photo-oxidation of synthetic groundwater saturated with DNAPL using hydrogen peroxide and persulfate.

The evaporation contribution to the disappearance of low molecular weight COCs in the reaction media is high. The contribution of COCs disappearance by evaporation during oxidation tests is more remarkable when using hydrogen peroxide as an oxidant. This is an expected behaviour considering the low conversion of this oxidant achieved under dark conditions (Fig. 2). Nonetheless, evaporation decreases when the number of chlorine atoms in the molecule increases for all the tests.

For comparison purposes, the resulting oxidation kinetic constants for all COCs (k_i) were compared with the values obtained for lumped HCHs (k_{HCHs}) during the photo-oxidation processes. Results are plotted in Fig. 5. Ratios k_i/k_{HCHs} higher than 1 indicate that the removal of other COCs is faster than that of HCHs, whereas values lower than 1 reveal that the elimination of HCHs is favoured.

The ratio k_i/k_{HCHs} decreases with increasing the molecular weight of COCs, regardless of the oxidant used. This again confirms that compounds with fewer chlorine atoms are more susceptible to being oxidized than HCHs in synthetic groundwater saturated with DNAPL. During the process with hydrogen peroxide, the removal of CB and DCBs is noticeable compared to HCHs and other COCs. TCBs present a similar degradation rate and tetraCBs show a value 0.6 times lower. These results are to be expected considering the contribution of the evaporation process in the removal of TCBs and tetraCBs, where the conversion of this process is higher than that of oxidation (Table 3). The degradation of PCXs is 2 times higher than HCHs and HeptaCHs are not removed. At this point, it is important to remember that the conversion of HCHs was very low (Fig. 1c) and, hence, the ratios are high despite the conversion not reaching 100% for any of the COCs (Fig. 3c).

Table 2
Oxidation kinetic constants.

COCs	kH_2O_2/Fe (min^{-1})	kH_2O_2/Fe/LED (min^{-1})	$kNa_2S_2O_8$/Fe (min^{-1})	$kNa_2S_2O_8$/Fe/LED (min^{-1})
CB	0.0028	0.0055	0.0027	0.0666
DCBs	0.0024	0.0043	0.0028	0.0319
TCBs	0	0.0010	0.0027	0.0301
TetraCBs	0	0.0004	0.0010	0.0131
PCXs	0	0.0017	0.0024	0.0145
HCHs	0	0.0010	0.0024	0.0048
HeptaCHs	0	0	0.0002	0.0030

On the other hand, the degradation rates resulting from the treatment with persulfate are more similar for DCBs and TCBs, being around 6 times higher than the removal rate of HCHs. Likewise, tetraCBs and PCXs show a similar ratio, 3 times higher than that of HCHs. The ratio for CB is 14 times higher, whereas the value for HeptaCHs is only 0.35 times lower. This means that compounds with less chlorine atoms are also more easily oxidised with persulfate, and COCs with more chlorine atoms than HCHs present a quite similar degradation rate. Overall, COCs degrade more rapidly when using persulfate, promoting the removal of all compounds in synthetic groundwater saturated with DNAPL. This behaviour could be directly related to the different mechanisms of both radicals to break C-H and C-Cl bonds explained above (Khan et al., 2017).

Hydrogen peroxide and persulfate are powerful oxidants that could contribute directly to removing COCs. For this reason, tests with each oxidant in the presence or absence of LED-vis light were developed. Specifically, the treatment of synthetic groundwater saturated with DNAPL was carried out by H_2O_2, $Na_2S_2O_8$, H_2O_2/LED and $Na_2S_2O_8$/LED. Results (not shown) confirm negligible differences relating to results shown in Fig. 4, which corroborate the role of the catalyst (ferrioxalate complex) in the generation of free radicals during the combined treatments (H_2O_2/ferrioxalate/LED-vis and $Na_2S_2O_8$/ferrioxalate/LED-vis).

To shed light on the amount of oxidant consumed in the removal of COCs during photo-oxidation processes, Fig. 6 shows the consumption of moles of oxidant vs fraction of COCs disappeared in the reaction media.

As expected, oxidant consumption increases with COCs conversion since more radicals are needed to attain the depletion of all pollutants. The conversion achieved (final $X_{COCs} = 0.54$) during the process with hydrogen peroxide is mainly due to the removal of COCs with low chlorine atoms in the molecule ($X_{CB} = 0.66$; $X_{DCBs} = 0.67$). However, the final values obtained with persulfate included the removal of all COCs (final $X_{COCs} = 0.94$) since the lowest conversion value obtained was 74% for HeptaCHs. At 420 min, the oxidation conversion of COCs was around 50% during the process with hydrogen peroxide, and 16.11 moles oxidant/moles COCs were consumed. A similar conversion was achieved with persulfate in 15 min, consuming 4.48 moles oxidant/moles COCs. This reveals that a lower oxidant consumption is required to attain the same conversion when using persulfate.

Nonetheless, the removal of HCHs and HeptaCHs was negligible at 420 min with hydrogen peroxide (Fig. 3c) and at 15 min with persulfate (Fig. 3d), and, hence, there is an unproductive consumption of oxidants. By increasing the operation time to 240 min with persulfate, a total conversion of COCs of 90% was achieved, including the removal of HCHs (70%) and HeptaCHs (50%), and 9.08 moles oxidant/moles COCs were used. This consumption is also lower than the required at the end of the treatment with hydrogen peroxide, and the conversion attained is higher (90.00 vs. 53.85%). Finally, conversion of COCs close to 100% was registered at the end of the process with persulfate, where the oxidant consumption was also lower than that required with hydrogen peroxide (12.81 vs. 16.11 mol oxidant/mol COCs). These results point out that there is a higher unproductive consumption of hydrogen peroxide during the treatment of synthetic groundwater saturated with DNAPL concerning using persulfate.

The degradation of HCHs and other COCs contained in DNAPL polluted groundwater by photo-assisted processes can lead to the formation of other organochlorine compounds, which can also be hazardous to human health and the environment (Khan et al., 2017). However, no chlorinated compounds from Table 1 were detected by GC/ECD or GC/MSD. Only traces of chlorophenols were observed, and the presence of hexachlorobenzene was discarded. Furthermore, the dechlorination grade at the end of the treatment, i.e., the number of chlorine atoms released as chloride ions during the process, was determined. This informs about the presence or absence of organochlorine compounds in the treated effluents. The concentration of chlorides was only measured for the photo-oxidation with persulfate since the conversion of HCHs

Table 3
Conversions calculated for oxidation and evaporation processes.

Process	CB			DCBs			TCBs			TetraCBs		
	X	$X_{oxidation}$	$X_{evaporation}$	X	$X_{oxidation}$	$X_{evaporation}$	X	$X_{oxidation}$	$X_{evaporation}$	X	$X_{oxidation}$	$X_{evaporation}$
H_2O_2/Fe	0.91	0.44	0.47	0.81	0.45	0.36	0.40	0.00	0.40	0.15	0.00	0.15
H_2O_2/Fe/LED	0.97	0.62	0.35	0.92	0.64	0.28	0.63	0.26	0.37	0.52	0.12	0.41
$Na_2S_2O_8$/Fe	0.90	0.42	0.48	0.81	0.51	0.30	0.77	0.52	0.25	0.61	0.26	0.35
$Na_2S_2O_8$/Fe/LED	1	0.96	0.04	0.97	0.94	0.03	0.98	0.95	0.03	0.96	0.90	0.06

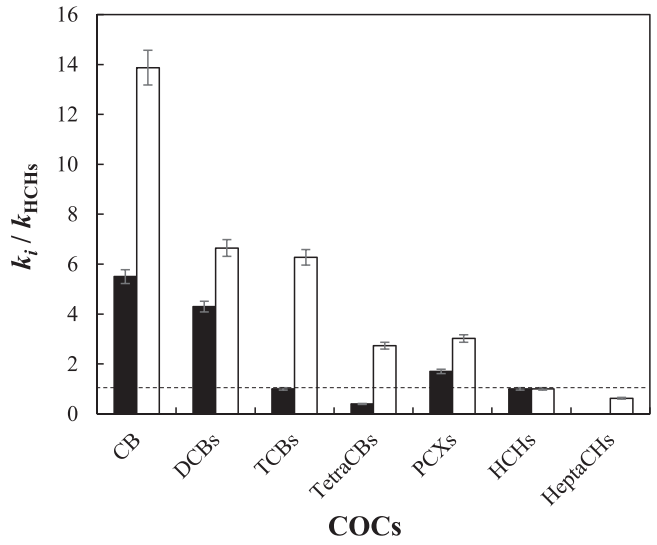

Fig. 5. Ratio k_i/k_{HCHs} as function of COCs during the photo-oxidation of groundwater saturated with DNAPL. (■) H_2O_2; (□) $Na_2S_2O_8$; $[Fe]_0$: 0.13 mM; $[H_2O_2]_0$: 7.5 mM; $[Na_2S_2O_8]_0$: 7.5 mM; I_{LED}: 0.18 W cm^{-2}; T: 25 ºC.

achieved with hydrogen peroxide was less than 40%. A final concentration of chlorides of 0.43 mM was obtained in the treated effluent, which corresponds to a dechlorination grade of 48.7% because the stoichiometric chloride concentration was 0.88 mM, considering the conversion achieved by oxidation in all COCs. Likewise, this process reduced the total organic carbon (TOC) from 65.42 to 42.84 mg L^{-1}, including the TOC associated to all COCs and the catalyst (ferrioxalate). These results suggest that using persulfate with ferrioxalate in the presence of LED-vis light removes COCs from DNAPL saturated groundwater and dechlorinates these pollutants.

4. Conclusions

The following conclusions can be drawn from this work:

- The photo-oxidation of DNAPL polluted groundwater using persulfate, ferrioxalate, and LED-vis light allows to remove HCHs up to 85%. Sulfate radicals are generated from persulfate activation with iron previously photo-activated by LED-vis light. These species promote the C-Cl bond cleavage of the molecule. The degradation rate of δ- and γ-HCH is higher than that of α- and ε-HCH because of the different solubility of the isomers.
- The use of hydrogen peroxide as an oxidant favours the production of hydroxyl radicals through the photo-Fenton reaction. The removal percentage of HCHs is less than 40%, regardless of the isomer evaluated with this oxidant. The mechanisms of hydroxyl radical to attack these pollutants seem to be the hydrogen abstraction or the hydroxyl addition, promoting the C-H bond cleavage. Furthermore, hydroxyl radicals are less selective than sulfate radicals; hence, the degradation efficiencies during the photo-Fenton process are lower.
- DNAPL polluted groundwater contains other COCs oxidized with both technologies, generating competitive oxidative reactions. The photo-Fenton process favours the elimination of low molecular weight compounds. In contrast, using persulfate with ferrioxalate under LED-vis light promotes the degradation of all COCs, reaching a total removal of most of them. The degradation rate of COCs with lower molecular weight than HCHs is higher. Still, HeptaCHs show a value similar to that of HCHs with persulfate and a negligible removal with hydrogen peroxide. COCs evaporation contributes to removing these pollutants from synthetic groundwater saturated with DNPL, and this process is significantly reduced when irradiating LED-vis light.
- A dechlorination grade close to 50% is obtained during the photo-oxidation with persulfate, confirming the ability of sulfate radicals to break the C-Cl bond in COCs, including HCHs.

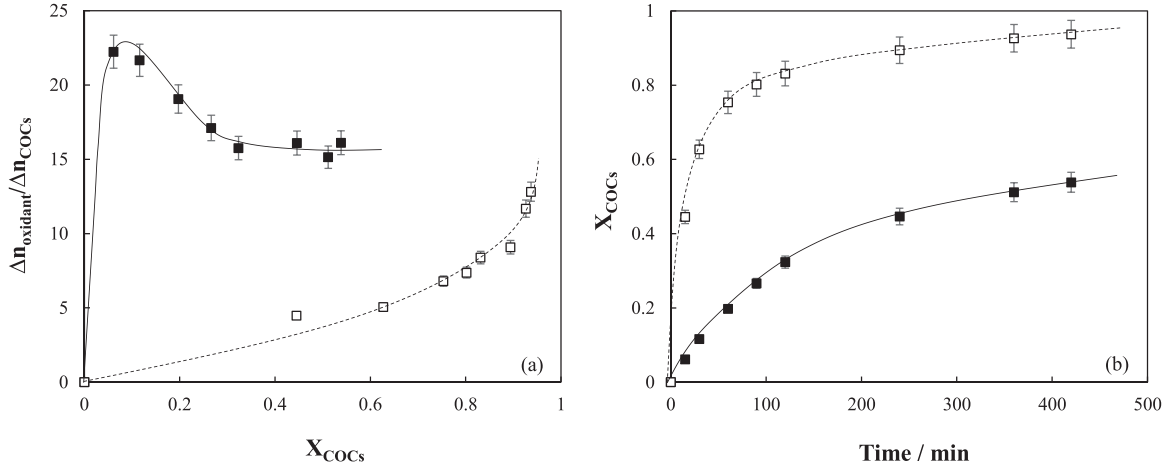

Fig. 6. (a) Consumption of oxidant as a function of the fraction of COCs removed during the photo-oxidation of groundwater saturated with DNAPL. (b) Conversion of COCs as a function of the operation time. (■) H_2O_2; (□) $Na_2S_2O_8$; $[Fe]_0$: 0.13 mM; $[H_2O_2]_0$: 7.5 mM; $[Na_2S_2O_8]_0$: 7.5 mM; $_{LED}$: 0.18 W cm^{-2}; T: 25 ºC.

Declaration of Competing Interest

The authors declare that they have no known competing financial interests or personal relationships that could have appeared to influence the work reported in this paper.

Acknowledgements

This research is part of the project PID2019-105934RB-I00 funded by MCIN/AEI/10.13039/501100011033 and project S2018/EMT-4317 (CARESOIL CM) funded by the Community of Madrid. Leandro O. Conte gratefully acknowledges the Marie Skłodowska-Curie Grant Agreement Nº 844209. Andrés Sánchez-Yepes also acknowledges the grant PRE2020-093195 funded by MCIN/AEI/10.13039/501100011033 and by "ESF Investing in your future".

References

Anipsitakis, G.P., Dionysiou, D.D., 2004. Radical generation by the interaction of transition metals with common oxidants. Environ. Sci. Technol. 38, 3705–3712.
Babuponnusami, A., Muthukumar, K., 2014. A review on Fenton and improvements to the Fenton process for wastewater treatment. J. Environ. Chem. Eng. 2, 557–572.
Birak, P.S., Miller, C.T., 2009. Dense non-aqueous phase liquids at former manufactured gas plants: challenges to modeling and remediation. J. Contam. Hydrol. 105, 81–98.
Campanale, C., Massarelli, C., Losacco, D., Bisaccia, D., Triozzi, M., Uricchio, V.F., 2021. The monitoring of pesticides in water matrices and the analytical criticalities: a review. TrAC Trends Anal. Chem. 144, 116423.
Carra, I., S.ánchez, Pérez, J.A., Malato, S., Autin, O., Jefferson, B., Jarvis, P., 2015. Application of high intensity UVC-LED for the removal of acetamiprid with the photo-Fenton process. Chem. Eng. J. 264, 690–696.
Conte, L.O., Querini, P., Albizzati, E.D., Alfano, O.M., 2014. Photonic and quantum efficiencies for the homogeneous photo-Fenton degradation of herbicide 2,4-D using different iron complexes. J. Chem. Technol. Biotechnol. 89, 1967–1974.
Conte, L.O., Schenone, A.V., Alfano, O.M., 2016. Photo-Fenton degradation of the herbicide 2,4-in aqueous medium at pH conditions close to neutrality. J. Environ. Manag. 170, 60–69.
Conte, L.O., Schenone, A.V., Giménez, B.N., Alfano, O.M., 2019. Photo-Fenton degradation of a herbicide (2,4-D) in groundwater for conditions of natural pH and presence of inorganic anions. J. Hazard. Mater. 113–120.
del Estado, B.O., 2018. Código de Aguas: Normativa Autonómica. España. Retrieved from http://www. boe. es/legislacion/codigos/codigo. php.
Díaz-Angulo, J., Cotillas, S., Gomes, A.I., Miranda, S.M., Mueses, M., Machuca-Martínez, F., Rodrigo, M.A., Boaventura, R.A.R., Vilar, V.J.P., 2021. A tube-in-tube membrane microreactor for tertiary treatment of urban wastewaters by photo-Fenton at neutral pH: a proof of concept. Chemosphere 263.
Díez, A.M., Ribeiro, A.S., Sanromán, M.A., Pazos, M., 2018. Optimization of photo-Fenton process for the treatment of prednisolone. Environ. Sci. Pollut. Res. 25, 27768–27782.
Dominguez, C.M., Checa-Fernandez, A., Romero, A., Santos, A., 2021. Degradation of HCHs by thermally activated persulfate in soil system: effect of temperature and oxidant concentration. J. Environ. Chem. Eng. 9, 105668.
Ebrahiem, E.E., Al-Maghrabi, M.N., Mobarki, A.R., 2017. Removal of organic pollutants from industrial wastewater by applying photo-Fenton oxidation technology. Arab. J. Chem. 10, S1674–S1679.
Eisenberg, G., 1943. Colorimetric determination of hydrogen peroxide. Ind. Eng. Chem. Anal. Ed. 15, 327–328.
Fernández, J., Arjol, M.A., Cacho, C., 2013. POP-contaminated sites from HCH production in Sabiñánigo, Spain. Environ. Sci. Pollut. Res. 20, 1937–1950.
Giannakis, S., Lin, K.Y.A., Ghanbari, F., 2021. A review of the recent advances on the treatment of industrial wastewaters by sulfate radical-based advanced oxidation processes (SR-AOPs). Chem. Eng. J. 406.
Graça, C.A.L., Velosa, A.Cd, Teixeira, A.C.S.C., 2017. Amicarbazone degradation by UVA-activated persulfate in the presence of hydrogen peroxide or Fe2. Catal. Today 280, 80–85.
Güler, C., 2019. Organic (hydrocarbon) contamination: nonaqueous phase liquids, GIS and geostatistical techniques for groundwater. Science 251–268.
Ioannidi, A., Arvaniti, O.S., Nika, M.C., Aalizadeh, R., Thomaidis, N.S., Mantzavinos, D., Frontistis, Z., 2022. Removal of drug losartan in environmental aquatic matrices by heat-activated persulfate: kinetics, transformation products and synergistic effects. Chemosphere 287.
Jiao, L., Zheng, G.J., Minh, T.B., Richardson, B., Chen, L., Zhang, Y., Yeung, L.W., Lam, J. C.W., Yang, X., Lam, P.K.S., Wong, M.H., 2009. Persistent toxic substances in remote lake and coastal sediments from Svalbard, Norwegian Arctic: levels, sources and fluxes. Environ. Pollut. 157, 1342–1351.
Khajone, V.B., Bhagat, P.R., 2020. Synthesis of polymer-supported Brønsted acid-functionalized Zn–porphyrin complex, knotted with benzimidazolium moiety for photodegradation of azo dyes under visible-light irradiation. Res. Chem. Intermed. 46, 783–802.
Khajone, V.B., Balinge, K.R., Patle, D.S., Bhagat, P.R., 2019. Synthesis and characterization of polymer supported Fe-phthalocyanine entangled with carboxyl functionalized benzimidazolium moiety: a heterogeneous catalyst for efficient visible-light-driven degradation of organic dyes from aqueous solutions. J. Mol. Liq. 288, 111032.
Khan, S., He, X., Khan, J.A., Khan, H.M., Boccelli, D.L., Dionysiou, D.D., 2017. Kinetics and mechanism of sulfate radical- and hydroxyl radical-induced degradation of highly chlorinated pesticide lindane in UV/peroxymonosulfate system. Chem. Eng. J. 318, 135–142.
Khan, S., Sohail, M., Han, C., Khan, J.A., Khan, H.M., Dionysiou, D.D., 2021. Degradation of highly chlorinated pesticide, lindane, in water using UV/persulfate: kinetics and mechanism, toxicity evaluation, and synergism by H2O2. J. Hazard. Mater. 402.
Kordestani, B., Jalilzadeh, Yengejeh, R., Takdastan, A., Neisi, A.K., 2019. A new study on photocatalytic degradation of meropenem and ceftriaxone antibiotics based on sulfate radicals: Influential factors, biodegradability, mineralization approach. Microchem. J. 146, 286–292.
Lian, L., Yao, B., Hou, S., Fang, J., Yan, S., Song, W., 2017. Kinetic study of hydroxyl and sulfate radical-mediated oxidation of pharmaceuticals in wastewater effluents. Environ. Sci. Technol. 51, 2954–2962.
Liang, C., Huang, C.F., Mohanty, N., Kurakalva, R.M., 2008. A rapid spectrophotometric determination of persulfate anion in ISCO. Chemosphere 73, 1540–1543.
Lorenzo, D., García-Cervilla, R., Romero, A., Santos, A., 2020. Partitioning of chlorinated organic compounds from dense non-aqueous phase liquids and contaminated soils from lindane production wastes to the aqueous phase. Chemosphere 239.
Lorenzo, D., Santos, A., Sánchez-Yepes, A., Conte, L.Ó., Domínguez, C.M., 2021. Abatement of 1,2,4-trichlorobencene by wet peroxide oxidation catalysed by goethite and enhanced by visible led light at neutral ph. Catalysts 11, 1–21.
Malato, S., Fernández-Ibáñez, P., Maldonado, M.I., Blanco, J., Gernjak, W., 2009. Decontamination and disinfection of water by solar photocatalysis: Recent overview and trends. Catal. Today 147, 1–59.
Matzek, L.W., Carter, K.E., 2016. Activated persulfate for organic chemical degradation: a review. Chemosphere 151, 178–188.
Mena, I.F., Cotillas, S., Díaz, E., Sáez, C., Rodríguez, J.J., Cañizares, P., Mohedano, Á.F., Rodrigo, M.A., 2018. Electrolysis with diamond anodes: eventually, there are refractory species! Chemosphere 195, 771–776.
Milh, H., Pessemier, J., Cabooter, D., Dewil, R., 2021. Removal of sulfamethoxazole by ferrous iron activation of persulfate: optimization of dosing strategy and degradation mechanism. Sci. Total Environ. 799.
Murov, S.L., Carmichael, I., Hug, G.L., 1993. Handbook of Photochemistry. CRC Press.
Neyens, E., Baeyens, J., 2003. A review of classic Fenton's peroxidation as an advanced oxidation technique. J. Hazard. Mater. 98, 33–50.
Nogueira, A.A., Souza, B.M., Dezotti, M.W.C., Boaventura, R.A.R., Vilar, V.J.P., 2017. Ferrioxalate complexes as strategy to drive a photo-FENTON reaction at mild pH conditions: A case study on levofloxacin oxidation. J. Photochem. Photobiol. A Chem. 345, 109–123.
Rao, Y., Long, H., Hao, J., 2021. The oxidative degradation of Caffeine in UV/Fe(II)/persulfate system—Reaction kinetics and decay pathways. Water Environ. Res. 93, 559–569.
Rodriguez, S., Vasquez, L., Costa, D., Romero, A., Santos, A., 2014. Oxidation of Orange G by persulfate activated by Fe(II), Fe(III) and zero valent iron (ZVI). Chemosphere 101, 86–92.
Rodriguez, S., Santos, A., Romero, A., 2017. Oxidation of priority and emerging pollutants with persulfate activated by iron: Effect of iron valence and particle size. Chem. Eng. J. 318, 197–205.
Santos, A., Fernández, J., Guadaño, J., Lorenzo, D., Romero, A., 2018. Chlorinated organic compounds in liquid wastes (DNAPL) from lindane production dumped in landfills in Sabiñanigo (Spain). Environ. Pollut. 242, 1616–1624.
Santos-Juanes, L., Amat, A.M., Arques, A., 2017. Strategies to drive photo-fenton process at mild conditions for the removal of xenobiotics from aqueous systems. Curr. Org. Chem. 21, 1074–1083.
Varanasi, L., Coscarelli, E., Khaksari, M., Mazzoleni, L.R., Minakata, D., 2018. Transformations of dissolved organic matter induced by UV photolysis, Hydroxyl radicals, chlorine radicals, and sulfate radicals in aqueous-phase UV-Based advanced oxidation processes. Water Res. 135, 22–30.
Wacławek, S., Lutze, H.V., Grübel, K., Padil, V.V.T., Černík, M., Dionysiou, D.D., 2017. Chemistry of persulfates in water and wastewater treatment: a review. Chem. Eng. J. 330, 44–62.
Wacławek, S., Silvestri, D., Hrabák, P., Padil, V.V.T., Torres-Mendieta, R., Wacławek, M., Černík, M., Dionysiou, D.D., 2019. Chemical oxidation and reduction of hexachlorocyclohexanes: a review. Water Res. 162, 302–319.
Wang, J., Wang, S., 2018. Activation of persulfate (PS) and peroxymonosulfate (PMS) and application for the degradation of emerging contaminants. Chem. Eng. J. 334, 1502–1517.
Wang, S.Y., Yang, Z.H., Lin, J.L., Lee, T.H., Kao, C.M., 2014. Site characterization and optimization of corrective actions at a chlorinated-solvent spill site. Adv. Mater. Res. 174–177.
Xiao, R., He, L., Luo, Z., Spinney, R., Wei, Z., Dionysiou, D.D., Zhao, F., 2020. An experimental and theoretical study on the degradation of clonidine by hydroxyl and sulfate radicals. Sci. Total Environ. 710.